

DEPARTMENT PROJECT I

PROJECT REPORT

Response Study of Electromagnetic Calorimeter



DEPARTMENT OF HIGH ENERGY PHYSICS
TATA INSTITUTE OF FUNDAMENTAL RESEARCH, MUMBAI

SUBMITTED BY: **Gursharan Singh**
SUPERVISED BY: **Dr Rajdeep Chatterjee**

30 JUNE 2024

Abstract

The Electromagnetic Calorimeter (ECAL) in the Compact Muon Solenoid (CMS) detector at the Large Hadron Collider (LHC) is crucial for measuring the energy of electrons and photons. The energy of these particles is reconstructed by the Superclustering algorithm. To study the variation in ECAL response, we performed an analysis using simulated electron samples. The response of the ECAL varies based on several factors, such as the transverse momentum of the electron, the position of the hit on the detector, and the shower shape variable R_9 . We have analyzed the comparison between the raw energy and the corrected energy response, and it is evident that the corrections applied improve the accuracy of the response.

Contents

1	Introduction	3
1.1	Electromagnetic Calorimeter (ECAL)	3
2	Response of ECAL	4
2.1	Intrinsic Factors	4
2.2	In-situ Factors	4
2.2.1	Algorithm Correction	5
3	Raw Energy	6
3.1	Correction Procedure	6
4	Corrected Energy	6
5	Comparison study of Energy Response of ECAL with Raw and Corrected Energy	7
5.1	Using Transverse Momentum	7
5.2	R_9	9
5.3	Energy Density ρ	10
5.4	Pseudorapidity η	11
6	Conclusion	12

1 Introduction

The Compact Muon Solenoid (CMS) detector is a general-purpose detector designed to study various physics processes, including both standard model processes and beyond standard model processes. Its primary objective upon its construction was the discovery of the Higgs boson, which was successfully achieved in 2012.

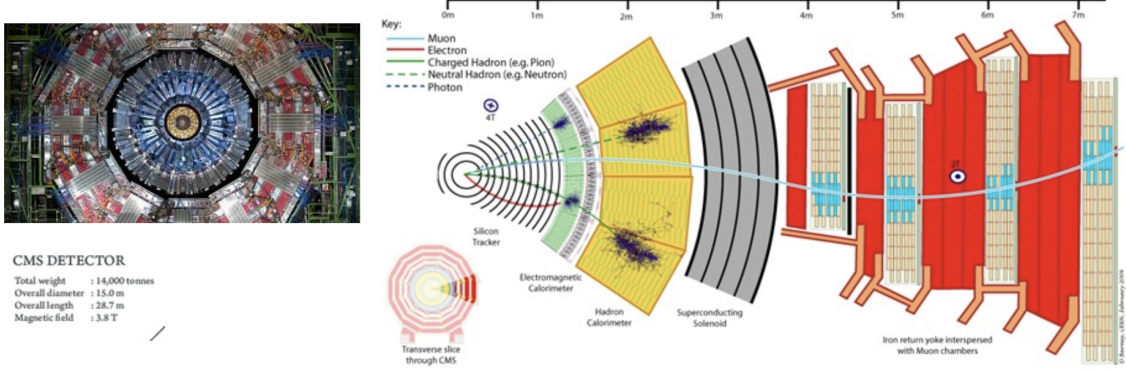


Figure 1: Different parts of the CMS detector.

1.1 Electromagnetic Calorimeter (ECAL)

In the CMS detector, we have an Electromagnetic Calorimeter (ECAL), which is designed primarily to detect Electromagnetic particles (e , γ) and measure their energies with high precision. The ECAL has a closed cylindrical geometry with a barrel and end caps. It consists of 75,848 lead tungstate (PbWO_4) crystals. These crystals span the barrel region (EB) ($|\eta| < 1.4$) to the end cap region (EE) ($1.5 < |\eta| < 3.0$). Here η , called pseudorapidity, is a spatial coordinate used to describe the angle of a particle relative to the beam axis. The barrel crystals have a front face cross-section of approximately $22 \times 22 \text{ mm}^2$ and a length of 230 mm, while the endcap crystals have a front face cross-section of $28.6 \times 28.6 \text{ mm}^2$ and a length of 220 mm.

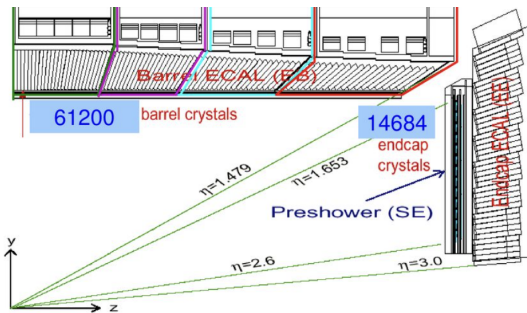


Figure 2: ECAL Section.

2 Response of ECAL

Response is defined as the relation between the radiation energy that fed to the detector and the total charge or the pulse height of the output signal that the detector measures. A good detector response has the following qualities:

1. Linearity: The response should be linear over the energy range of interest, meaning energy observed from the detector (E_{obs}) should be directly proportional to the energy given to the detector (E_{gen}).
2. Stability: The response should be stable over time, ensuring consistent performance and accuracy.

As discussed earlier ECAL measures energy of mainly (e,γ) so its response should be defined as the $\frac{E_{obs}(e,\gamma)}{E_{gen}(e,\gamma)}$.

2.1 Intrinsic Factors

The ECAL intrinsic energy [2] response has been measured as follows:

$$\frac{\sigma_E}{E} = \frac{a}{\sqrt{E}} \oplus \frac{b}{E} \oplus c$$

where a,b, and c are constants.

The First term a is called a stochastic term that arises due to the statistical nature of the energy deposition process. Hence, it's a number-counting term that is because of Poisson statistics.

The second term b is called the noise term which arises due to several reasons like electronic noise, pile-up, etc

The third term c is the constant term, it arises due to reasons like the non-uniformity of the longitudinal scintillation light collection and the energy leakage from the back of the crystals, energy deposit in the dead areas, etc.

2.2 In-situ Factors

The following are the in-situ factors that are responsible for the Response:

1. Stability of the time response correction of the crystals
2. Accuracy of the inter-crystal calibration
3. Accuracy of the algorithm for correction to the energy that has been derived based on the simulations

Crystals have lost their transparency due to the radiation from the collision, hence output yield of crystals is not stable with time. To correct this, there is a laser-monitored system, which after every 40 min shoots the laser pulses to the crystals and the pin diode (used as reference) through which corrections are measured.

2.2.1 Algorithm Correction

The entire summary of work started from section 2.2 to section 4 is derived from the paper [1].

Offline electron and photon reconstruction: Electrons and photons are particles that interact via electromagnetic interactions, causing them to interact with the medium before depositing their energy in the ECAL. Electrons, due to their high energy, undergo bremsstrahlung when decelerating through material interactions, producing photons as they travel. If these photons have energy greater than 1.02 MeV, they can lead to pair production in the presence of material nuclei. Consequently, a single object can reach the ECAL as an electromagnetic shower, containing numerous electrons and photons.

Electrons, being charged particles, deflect from their original path in the presence of a magnetic field due to the Lorentz force, and this deflection is detected by the tracker. The tracker material often causes the early development of electromagnetic showers, making it challenging to identify electrons and photons solely based on ECAL hits.

The reconstruction of (e, γ) energy for the ECAL has the following steps :

- **Step 1 - Identifying Crystals :** As stated above the (e, γ) object produces an electromagnetic shower that hits various places to the ECAL crystals, so the first process of the reconstruction is to identify the crystals having energy deposited that exceeds a predefined threshold (80MeV for EB and 300MeV for EE), this threshold is designed to avoid noise so it's mainly 2 to 3 times higher than the electronic noise expected in the crystals. Then, out of these crystals, with transverse energy of 1GeV are called Seed crystals. We start our clustering around them until we reach the non-selected crystals.
- **Step 2 - Clustering the Clusters:** Now we have many clusters as there are many hits that act like seed crystals. These clusters together combine to form a big group of clusters called a **Supercluster[1]** (SC), one supercluster corresponds to a prompt (e, γ) object.
- **Step 3 - Superclustering in the ECAL:**
 1. The first is the "Mustache" Algorithm, which is very useful for low-energy deposits in ECAL. It first identifies the cluster above a given threshold called seed cluster and adds other clusters that fall into the area that appears mustache in shape in the transverse plane to form a Supercluster. The distribution of the $\Delta\eta = (\eta_{\text{seed cluster}} - \eta_{\text{cluster}})$ vs $\Delta\theta = (\theta_{\text{seed cluster}} - \theta_{\text{cluster}})$ is bending because of the magnetic field of the CMS solenoid. The size of the mustache region depends upon the transverse energy (E_t), if (E_t) is more, it bends less in a magnetic field, and vice versa.
 2. After the first algorithm, some clusters are still not included in the supercluster, so it uses tracking information to extrapolate bremsstrahlung tangents and conversion tracks to decide whether a cluster should belong to a particular SC or not, this is called refined superclustering.

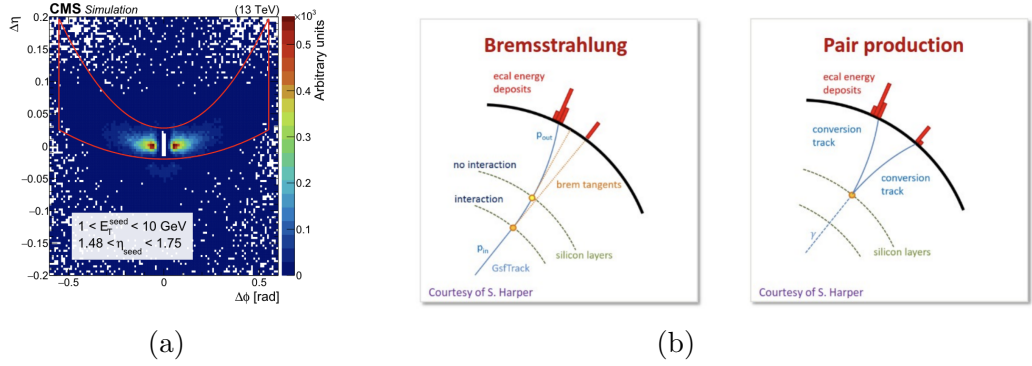


Figure 3: (a) is the Mustache curve, used for superclustering. (b) is the method to recover lost Bremsstrahlung photons and Pair production electrons in the refined algorithm.

3 Raw Energy

The energy obtained by the Supercluster is called the raw energy, as it still has many corrections that need to be added. The following are the losses that raw energy does not include:

1. Energy lost in gaps
2. Energy lost in large amount of upstream material in front of ECAL.
3. Pile up

3.1 Correction Procedure

Using a regression model of Boosted Decision Trees (BDT), a machine learning algorithm, the raw energy is corrected. The target variable is the ratio of generator level (e, γ) energy to the raw SC energy. The input variables are the SC position and shower shape variables which tell about the degree of showering in the material, and the location of photon conversion. Finally, with the number of reconstructed vertices and median energy density in the event, we included the correct residual energy scale effect from the pileup.

For testing the goodness of regression [BDT] we used $Z \rightarrow e^+e^-$ samples and applied the same BDT model and built Z peak from it, as we know the correct Z peak should have a mass around $91.18 \text{ GeV}/c^2$.

4 Corrected Energy

After the corrections applied by the BDT to the raw energy we got the Corrected Energy, which included the corrections corresponding to

1. Energy loss in the material in front of ECAL
2. Intermodule gaps or dead crystals
3. Effects of pileup

5 Comparison study of Energy Response of ECAL with Raw and Corrected Energy

Using the simulated data of electrons, we studied the response of the barrel region of the ECAL.

We did the variable binning to maintain the equal statistics of data in each bin, after this we took each bin's data and calculated the response, which is $\frac{E_{\text{raw}}}{E_{\text{gen}}}$ for raw energy and similarly corrected energy $\frac{E_{\text{Corrected}}}{E_{\text{gen}}}$.

Now we fitted each bin data using a Cruijff function which is defined as follows:

$$f(x; m_0, \sigma_L, \sigma_R, \alpha_L, \alpha_R) = \begin{cases} \exp\left(-\frac{(x-m_0)^2}{2(\sigma_L^2 + \alpha_L(x-m_0)^2)}\right) & \text{if } x < m_0 \\ \exp\left(-\frac{(x-m_0)^2}{2(\sigma_R^2 + \alpha_R(x-m_0)^2)}\right) & \text{if } x \geq m_0 \end{cases}$$

We tried the Gaussian function (Fig.4 (a)) as well, but it was not able to fit the data well, so we chose the Cruijff function (Fig.4 (b)).

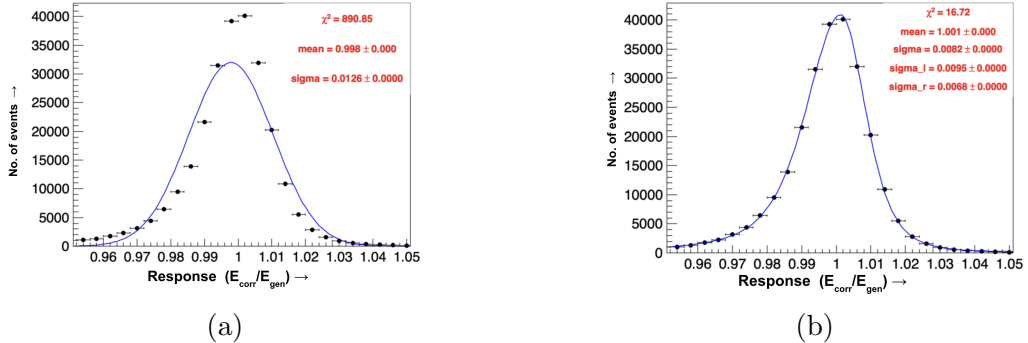


Figure 4: (a) and (b) are the R_9 corrected energy response plots in bin 0.98-0.99 of the R_9 distribution fitted with Gaussian and Cruijff functions respectively.

5.1 Using Transverse Momentum

We have the flat distribution for the Transverse momentum of the electron. So we slice the distribution into 20GeV bins from 20GeV to 300GeV, here we have taken equal bin width as the distribution is flat in nature, so there are equal statistics in each bin.

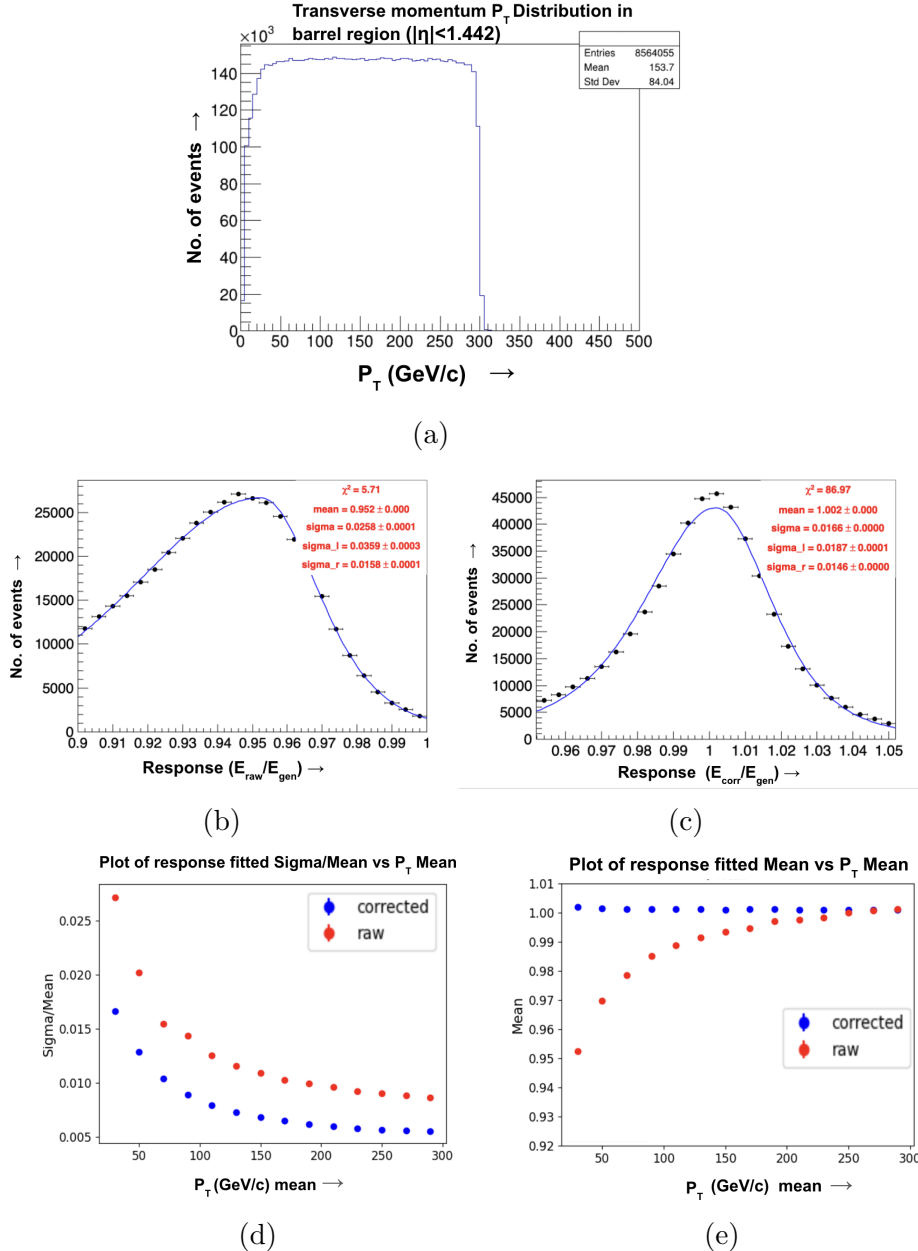


Figure 5: (a) is the Transverse momentum P_T distribution of electrons in the barrel region ($|\eta| < 1.442$). (b) and (c) are the fitted energy response in bin 20-40 GeV/c of P_T distribution with cruijff function for raw and corrected energy respectively. (d) and (e) is the comparative plot of relative energy resolution and energy mean of the response with mean P_T values.

The reason for the behavior in Fig. 5 (d) is that at high P_T , the particle bends less in the magnetic field, making the recovery of bremsstrahlung photons easier. Similarly, in Fig. 5 (e), at lower P_T , it loses more energy due to bremsstrahlung, and the corrected plot shows a straight line as we have accounted for this lost energy.

5.2 R_9

It is defined as the ratio of the energy contained in the 3x3 array of crystals centered around the crystal with the highest energy deposit (the seed crystal) to the total energy of the supercluster i.e $R_9 = \frac{E_{3\times 3}}{E_{\text{Supercluster}}}$.

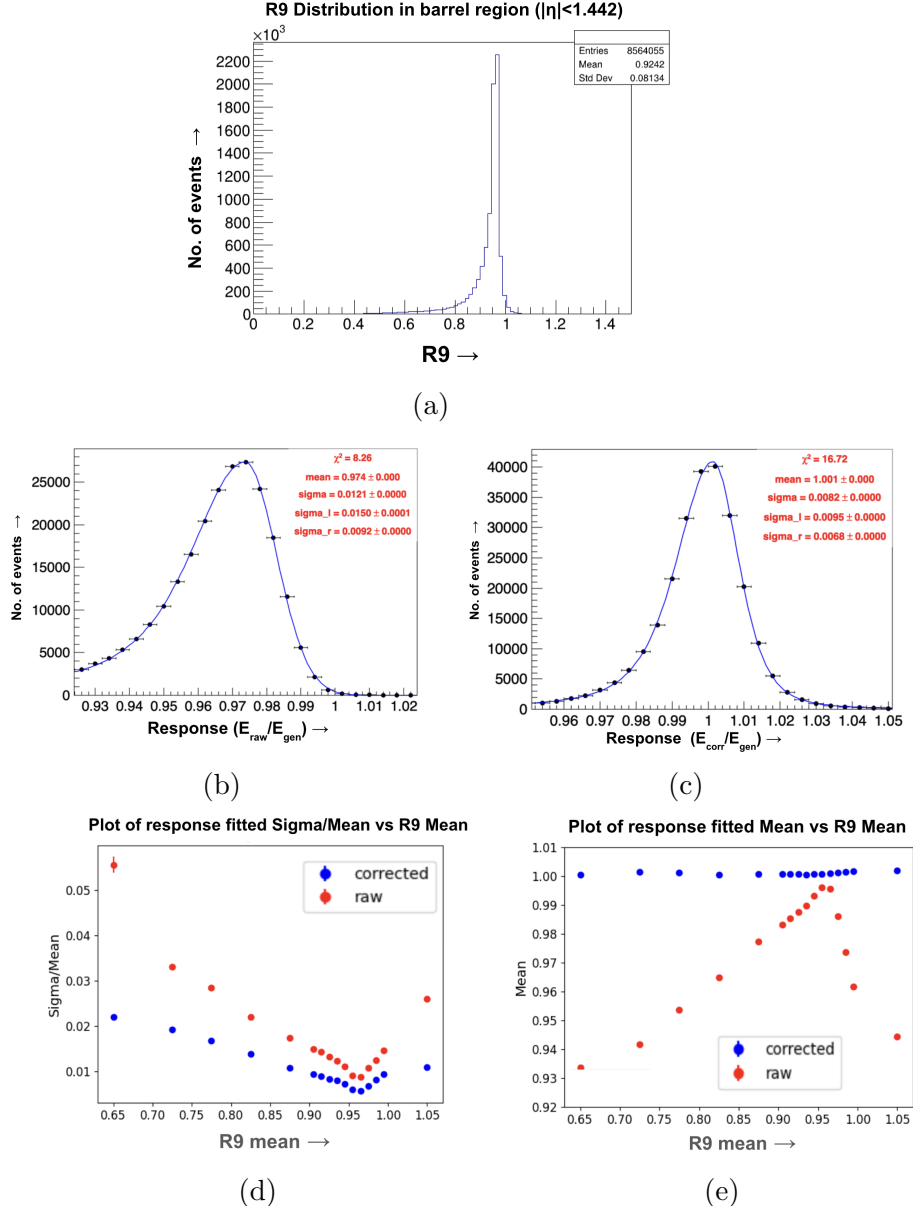


Figure 6: (a) is the R_9 distribution of electrons in the barrel region ($|\eta| < 1.442$). (b) and (c) are the fitted energy response in bin 0.98-0.99 of the R_9 distribution with cruijff function for raw and corrected energy respectively. (d) and (e) is the comparative plot of relative energy resolution and energy mean of the response with mean R_9 values.

With R_9 , the relative response in Fig.6(d) decreases, while the raw energy response mean in Fig.6(e) increases. This occurs because as R_9 increases, electrons

exhibit less showering, leading to less loss of bremsstrahlung photons.

5.3 Energy Density ρ

Energy Density (ρ) is defined as the energy that is due to soft interaction (the interaction not of our interest), so its the avoidable energy that we are getting. Higher (ρ) values indicate a higher number of pileup interactions.

Here we have a decreasing nature of the distribution, so we applied variable binning, such that each bin has sufficient statistics.

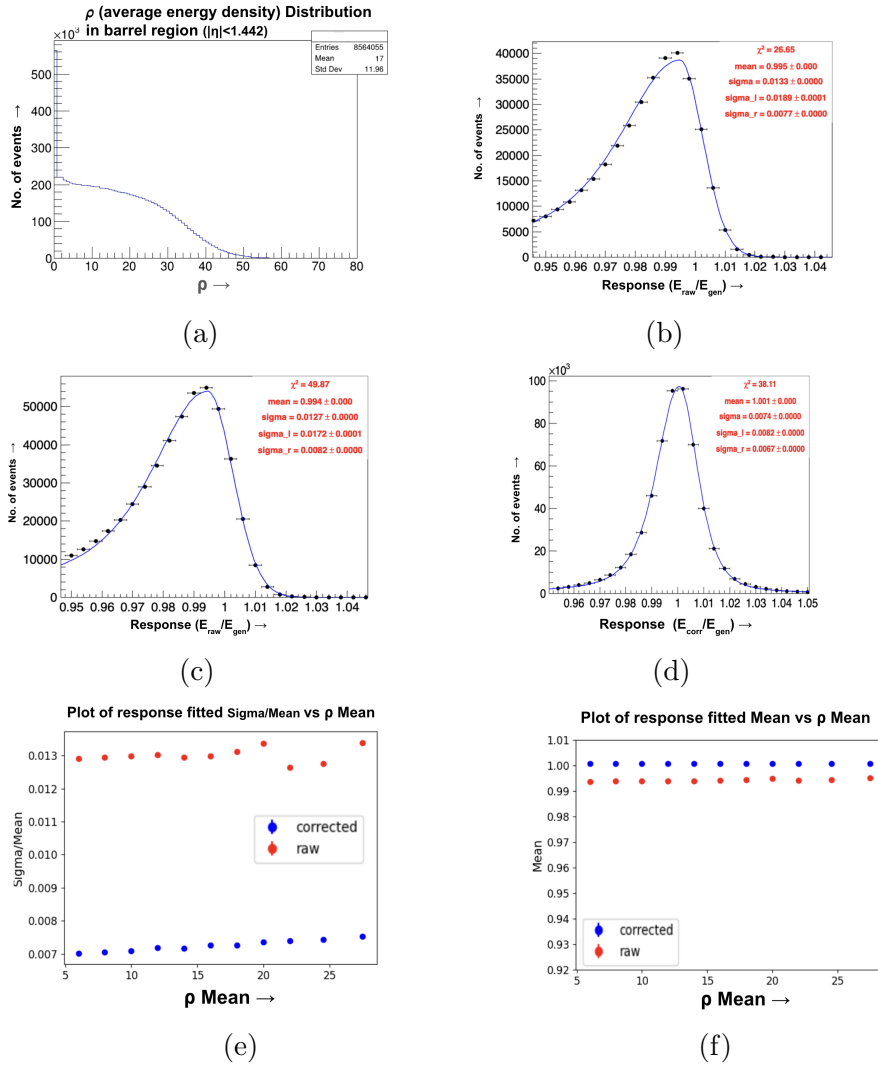


Figure 7: (a) is the energy density (ρ) distribution of electrons in the barrel region ($|\eta| < 1.442$). (b) is the fitted energy response in bin 19-21 of the ρ distribution with cruijff function for raw energy. (c) and (d) are the fitted energy response in bin 23-26 of the ρ distribution with cruijff function for raw and corrected energy respectively. (e) and (f) is the comparative plot of relative energy resolution and energy mean of the response with mean ρ values.

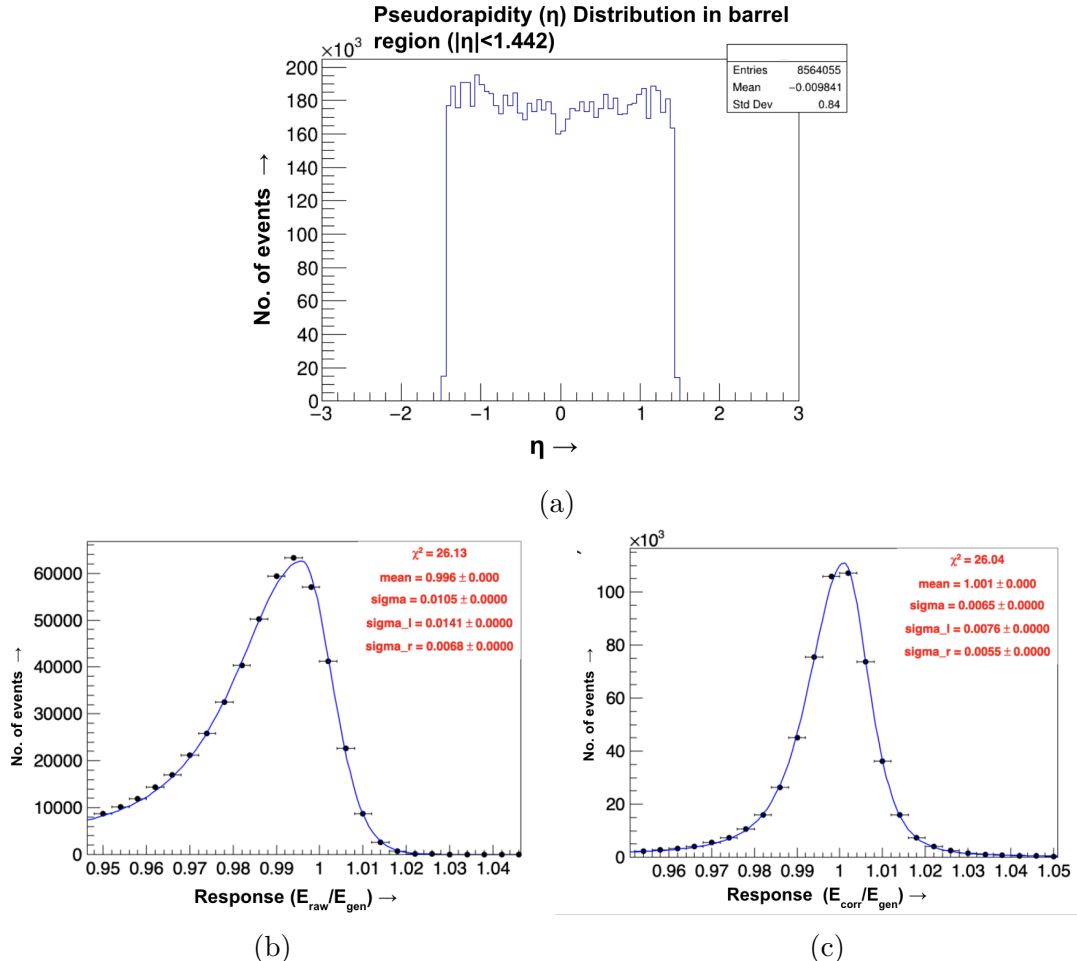
The reason for behavior of increasing raw energy in Fig.7 (e) with higher values of ρ is simply more number of pileup interactions that are degrading the relative resolution.

The sudden change in the raw energy response nature between ρ values of 20-25 is attributed to poor histogram fitting, evident from the increasing chi-square values observed for raw energy from (b) to (c).

In the corrected scenario, the response should ideally be flat. However, it still shows an increasing trend, which may indicate that our correction algorithms are not fully efficient.

5.4 Pseudorapidity η

Pseudorapidity η is a spatial coordinate used to describe the angle of a particle relative to the beam axis. It is defined as : $\eta = -\ln \tan \frac{\theta}{2}$, where θ is the polar angle relative to the beam axis. Here also as the distribution is flat in η so we did equal width binning from -1.4 to 1.4 in 0.2 bins.



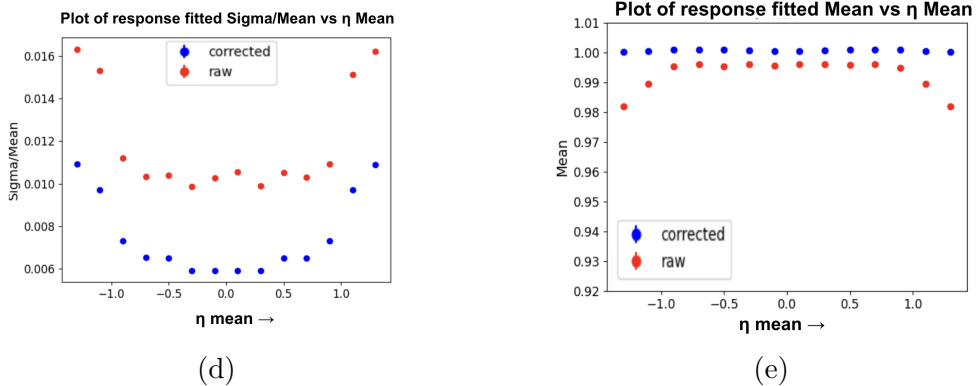


Figure 8: ((a) is the Pseudorapidity (η) distribution of electrons in the barrel region ($|\eta| < 1.442$). (b) and (c) are the fitted energy response in bin of 0.4-0.6 of (η) distribution with cruijff function for raw and corrected energy respectively. d) and (e) is the comparative plot of relative energy resolution and energy mean of the response with mean (η) values.

In Fig. 8 (d), the value is lowest at $\eta = 0$ because there is very little tracker material present in that region. As we move to either side of η , the amount of tracker material symmetrically increases, causing electrons to lose more energy in the tracker medium. Additionally, in Fig. 8 (e), the raw energy decreases on either side at the extreme ends due to more interactions with the tracker material, leading to energy losses.

6 Conclusion

We have observed that the response of E_{Raw} vs $E_{\text{Corrected}}$ varies significantly across different parameters, with $E_{\text{Corrected}}$ exhibiting comparatively lower relative resolution of response of ECAL. Therefore, all the corrections applied to $E_{\text{Corrected}}$ effectively enhance our detector's response.

Acknowledgements

I would like to thank Dr. Rajdeep Chatterjee for guiding me at each step of this project. I am grateful to Prof. Gobinda Majumder for helping me understand the plotting and fitting of histograms. I also wish to thank Dr. Shilpi Jain for her assistance in discussing the problems related to this project.

References

- [1] Electron and photon reconstruction and identification with the cms experiment at the cern lhc. *Journal of Instrumentation*, 16(05):P05014, May 2021.
- [2] İlhan Tapan and Fatma Kocak. A study on stochastic term of calorimetric energy resolution. *Journal of Physics: Conference Series*, 293:012030, 05 2011.